INTERNATIONAL SOCIETY FOR SOIL MECHANICS AND GEOTECHNICAL ENGINEERING

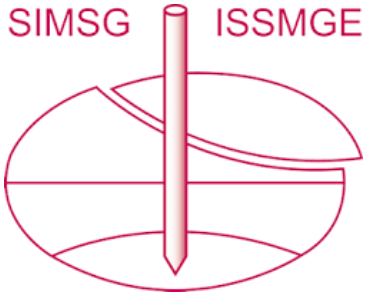

This paper was downloaded from the Online Library of the International Society for Soil Mechanics and Geotechnical Engineering (ISSMGE). The library is available here:

https://www.issmge.org/publications/online-library

This is an open-access database that archives thousands of papers published under the Auspices of the ISSMGE and maintained by the Innovation and Development Committee of ISSMGE.

The paper was published in the proceedings of the 7th International Young Geotechnical Engineers Conference and was edited by Brendan Scott. The conference was held from April 29th to May 1st 2022 in Sydney, Australia.

Proceedings of the 7th International Young Geotechnical Engineers Conference – Scott (Ed.)
© 2022 Australian Geomechanics Society, Sydney Australia, ISBN 978-0-9946261-5-8

Excess pore pressure estimation based on cyclic laboratory tests

Estimation des pressions interstitielles excessives sur des tests cycliques en laboratoire

Jann-Eike Saathoff & Martin Achmus
Institute for Geotechnical Engineering, Leibniz University Hannover, Germany, saathoff@igth.uni-hannover.de

ABSTRACT: In particular during storm events, an accumulation of excess pore pressures may occur in the soil around cyclically loaded offshore foundations for systems with partial or no dissipation between adjacent load events. The pore pressure build-up reduces the effective stresses in the soil and may negatively affect the structural integrity of offshore foundations. The excess pore pressure build-up for a specific soil is a highly non-linear function and currently there is no simple concept to estimate a sufficient number of laboratory tests and their boundary conditions. In the following, the results of an extensive displacement-controlled direct simple shear test program are investigated. The findings have been compared with the shear strain threshold concept and different thresholds have been identified. As a main result, an optimal laboratory program can be derived based on a more detailed understanding of the soil response under strain-controlled conditions. The overall soil response can easily be derived based on the shear strain threshold concept in a combination with Resonant Column and multistage direct simple shear testing and either be used with a linearized or an advanced excess pore pressure estimation equation.

RÉSUMÉ: En particulier pendant les tempêtes, une accumulation de pressions interstitielles excessives peut se produire dans le sol autour des fondations offshore soumises à des charges cycliques pour les systèmes avec une dissipation partielle ou nulle entre les événements de charge adjacents. L'accumulation de la pression interstitielle réduit les contraintes effectives dans le sol. Elle peut avoir un effet négatif sur l'intégrité structurelle des fondations offshore. L'accumulation de la surpression interstitielle pour un sol spécifique est une fonction hautement non linéaire. Il n'existe actuellement aucun concept simple pour estimer un nombre suffisant d'essais en laboratoire et leurs conditions limites. Dans ce qui suit, les résultats d'un vaste programme d'essais de cisaillement simple direct contrôlé par le déplacement ont été étudiés. Les résultats ont été comparés au concept de seuil de déformation en cisaillement et différents seuils ont été identifiés. Le principal résultat obtenu est un programme de laboratoire optimal basé sur une compréhension plus détaillée de la réponse du sol dans des conditions de déformation contrôlée. La réponse globale du sol peut facilement être dérivée sur la base du concept de seuil de déformation en cisaillement en combinaison avec la colonne résonante et les essais de cisaillement simple direct en plusieurs étapes. Elle peut être utilisée avec une équation d'estimation de l'excès de pression interstitielle linéarisée ou avancée.

KEYWORDS: Monopiles; cyclic loading; excess pore pressure; liquefaction; strain-controlled.

1 INTRODUCTION

The accurate estimation of excess pore pressure is not only essential in earthquake engineering but does also play a major role when dealing with offshore foundations. The loads acting on offshore foundations are highly variable and therefore to be considered cyclical. Cyclic loads can lead to an accumulation of excess pore water pressures in sandy soils, especially during a storm event. The build-up of excess pore pressures and hence partial or full liquefaction can influence the integrity of the overall offshore structure.

The capacity, as well as the serviceability, is at risk if (partial) liquefaction occurs. Liquefaction can be induced either by earthquakes or cyclic loading in case of partial or no dissipation between adjacent load events. Cyclic shearing leads to an increase in excess pore pressure and subsequently to a reduced grain-to-grain contact. This build-up mechanism of excess pore pressure is accompanied by an accumulation effect over a specific number of cycles in which the absolute excess pore pressure cannot fully dissipate and hence may increase gradually due to accumulation.

The potential of excess pore pressure build-up is usually investigated with cyclic triaxial and cyclic direct simple shear tests (DSS). Instead of true undrained tests, constant volume tests on dry samples are often performed in practice when using the common direct simple shear tests. In constant-volume tests, the initial vertical stress decreases over the number of cycles, because of a contractive soil behaviour. The contractive behaviour needs to be adjusted for with a decrease in vertical stress to fulfil the constant-volume boundary conditions. This decrease, determined on a dry sample, can approximately be interpreted as the increase in excess pore water pressure of a fully saturated sample within a truly undrained test (Feda 1971, Finn et Vaid 1977, Dyvik et al. 1987).

The excess pore pressure build-up for a specific soil is a function of stress, the number of cycles and the cyclic shear strain amplitude. This function is highly non-linear. There is currently no simple concept to estimate a sufficient number of laboratory tests and their boundary conditions to meet the requirements for an accurate representation of soil response. In order to accurately assess the soil response, many different tests for different cyclic shear strains amplitudes are necessary. These test can be used to estimate the non-linearity needed in the design calculations. A simple estimation approach can reduce the amount of tests and simultaneously help to understand the soil response of displacement-controlled test ever further.

In the following, the soil response for displacement-controlled direct simple shear tests is presented and evaluated to capture the complex cyclic soil response by using the shear strain threshold concept (Vucetic 1994). The function can be used in conjunction with explicit methods in order to derive the behaviour of offshore foundation due to cyclic loading (Achmus et al. 2018, Saathoff et Achmus 2020).

2 STATE OF THE ART

Figure 1 shows a typical result for a cyclic displacement-controlled element test with the hysteresis of the first cycle and a hysteresis after several number of cycles. For a sheared specimen, the initial soil stiffness appears to be the initial shear modulus G_0. This shear modulus is also expected at the beginning of load-reversal. The hysteresis can be characterized with the secant shear modulus defined by the quotient of the shear stress

and shear strain at the end of points of each cycle. For displacement-controlled cyclic tests the shear strain amplitude remains constant and the shear stress generally decreases over the number of cycles (grey curve in Figure 1). This leads to a decreased shear modulus G_N. The soil response is softer after several cycles depending on the applied cyclic shear strain amplitude.

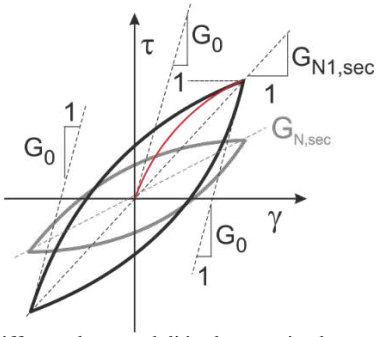

Figure 1. Different shear moduli in shear strain-shear stress hysteresis from cyclic element tests.

2.1 *Shear modulus degradation*

When a specimen is sheared the soil response gets softer with increasing deformation. This behaviour can clearly be seen within the shear modulus degradation curve. The shear modulus degradation curve is normalized by the initial shear modulus. For very small shear strains, the stress-dependent initial shear modulus G_0 is obtained (Figure 1, Figure 2). The subsequent reduction can be roughly categorized by four threshold values. The first shear strain threshold value γ_{tl} marks the end of the absolute linear elastic and the beginning of the nonlinear response up to the second threshold. The linear threshold can be read from results from Resonant Column tests at 0.99 G/G_0 (Vucetic 1994). It represents the region in which very small shear strains occur and the soil responses are quasi-linear elastic. The shear strains found in the literature vary from 5E-6 to 6E-5 (Wichtmann et Triantafyllidis 2010, 2013).

The second value is the volumetric threshold γ_{tv} below which no significant plastic volumetric strain or excess pore pressure accumulation can be expected. The volumetric threshold represents the transition from intermediate-strains to irrecoverable deformation and small changes in the soil skeleton. A shear strain smaller than the volumetric threshold lies in the nonlinear elastic region including no sliding of grain-to-grain; from there on mainly nonlinear-plastic response can be expected (Dobry et al. 1982, Silver et Seed 1971).

For larger shear strains than the volumetric threshold shear strain, other threshold definitions for sand and clay can be found in the literature. Additional thresholds, namely the cyclic threshold for cyclic degradation and the cyclic threshold for cyclic excess pore water pressure or thresholds for cyclic settlement or cyclic stiffening, are furthermore differentiated (Vucetic and Mortezaie 2015). All these try to categorize the soil response based on a general change of the microstructural mechanisms or the softening of the soil response due to a reduction of effective stresses by means of an increased excess pore pressure. Such a detailed categorization between mechanical abrasion effects and excess pore pressure build-up shall not be done in following. Any cyclic degradation of the soil is equated with a softened soil response and a build-up of excess pore pressure. The degradation threshold defines the softening of the soil sample in a simplified way.

At the degradation threshold γ_{td} the shear modulus starts to decrease rapidly. In order to show that the degradation threshold is interpreted from the authors' point of view, it is marked with a tilde as $\tilde{\gamma}_{td}$.

In case of cyclic loading, the shear strain can be interpreted as the shear strain amplitude. For cyclic loading a larger decrease of the soil stiffness with an increasing number of cycles is expected. However, there is no clear definition for the degradation threshold. It is interpreted as the transition to irreversible changes in the microstructure and the beginning of an unstable cyclic behaviour. For shear strains amplitudes smaller than $\tilde{\gamma}_{td}$ the shear modulus does not decrease with increasing number of cycles. This is not the case for larger shear strains as there is mainly a plastic response for the degradation threshold $\tilde{\gamma}_{td}$ and the flow threshold γ_{tf} (Okur and Ansal 2007).

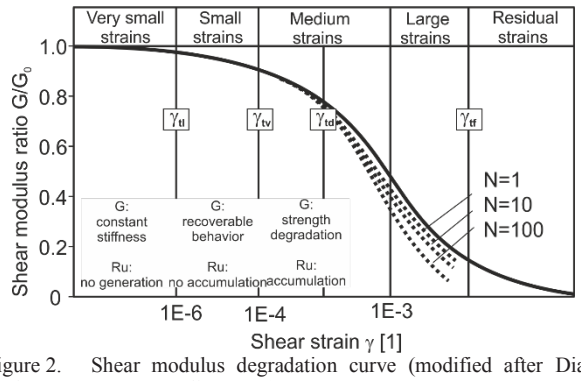

Figure 2. Shear modulus degradation curve (modified after Diaz-Rodríguez et Lopez-Molina 2008).

2.2 *Excess pore pressure estimation*

The different soil responses at different shear strains is combined with a liquefaction analysis. Seed (1976) describes liquefaction as a flow state in which due to high excess pore pressures only a small resistance of the soil element is present and the element phase-transforms from solid to liquid. Subsequently, a continuous deformation of the soil element occurs. Usually, the excess pore pressure Δu is normalized by the effective vertical stress to the normalized excess pore pressure R_u in case of an one-dimensional boundary conditions (direct simple shear test):

$$R_u = \frac{\Delta u}{\sigma'_v} \qquad (1)$$

For three-dimensional conditions (as of triaxial test, cf. Figure 3), the octahedral stress, which is the mean stress of all principal stresses, is used for normalization:

$$R_u = \frac{\Delta u}{\sigma'_{oct}} \qquad (2)$$

Liquefaction is often defined as the state where the permanent normalized excess pore pressure reaches 0.95.

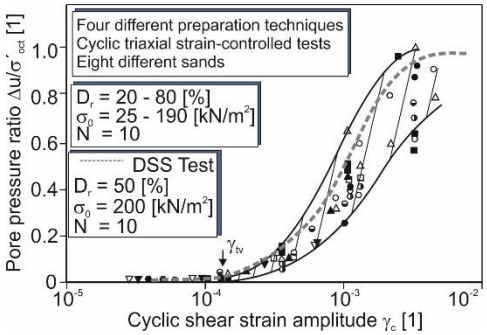

Figure 3. Excess pore pressure build-up in different sands in cyclic triaxial strain-controlled test (Dobry et al. 1985) and comparison with results from DSS tests carried out by the authors for N=10 and S30T sand.

The most common strain-based approach when dealing with liquefaction was published by Dobry et al. (1982) based on isotropic consolidated cyclic triaxial tests. They correlate the

excess pore pressure directly to the shear strain amplitude. The volumetric strain threshold γ_{tv} defines herein the minimum shear strain amplitude for which no accumulation of excess pore pressure occurs. Figure 3 shows the normalized excess pore pressure against the cyclic shear strain amplitude for different octahedral stresses and void ratios. Additionally, different sands and preparation techniques are included. Dobry et al. (1982) state that the build-up of excess pore pressure is, regarding the bandwidth in Figure 3, mostly independent of the confining pressure and sample preparation.

3 LABORATORY TESTS

Different laboratory tests have been performed on non-cohesive soils. A poorly-graded quartz sand termed "S30T" was investigated with different relative densities. The sand shows a grain size distribution typical for North Sea conditions and a relative density of $D_r = 0.85$ was chosen as a reference case. The soil properties for the reference soil are shown in Table 1. Several additional soils have been investigated to show the influence of the grain size distribution and particle shape, but only the results for the reference soil will be discussed in the following. A microscopic image in order to assess the grain shape is depicted in Figure 4.

Table 1. Soil parameters for reference sand S30T.

e_{max} [1]	e_{min} [1]	d_{10} [mm]	d_{50} [mm]	d_{60} [mm]	ρ_s [g/cm³]
0.789	0.493	0.256	0.347	0.461	2.65

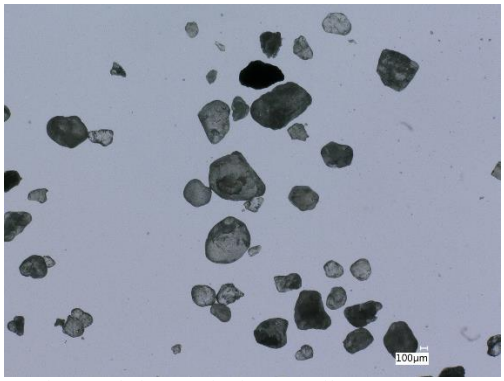

Figure 4: Microscopic image of reference soil.

Several cyclic direct simple shear tests in a constant volume procedure were carried out. The direct simple shear device of GDS Instruments with a local high-resolution shear strain LVDT was used. The general soil response has been investigated for six different vertical stresses in the range from 50 kPa to 600 kPa with cyclic shear strain amplitudes between 0.005% to 5%. In total over 300 tests with different parameters with up to 100.000 cycles were performed. Overall, the strain-controlled test procedure offers several advantages in terms of repeatability and accuracy (Dobry et al., 1985). Figure 3 shows a comparison between the soil response for a vertical stress of 200 kPa and 10 cycles in a cyclic direct simple shear test with the results obtained by Dobry et al. (1985) for eight different sands and with varying relative density and octahedral stress. The general trend, as well as the volumetric threshold, fit quite well. Liquefaction is reached at a cyclic shear strain amplitude of approximately 0.4%. This value depends on the vertical stress and the number of cycles, which will be discussed later.

The soil response is independent of the mean shear strain. This is illustrated by Figure 5, which was derived from a matrix of nine strain-controlled cyclic DSS tests. The governing parameters are the number of cycles, the cyclic shear strain and the confining pressure. This is in contrast to load-controlled tests in which two-way loads induce higher excess pore pressures than one-way loads with the same amplitude.

Depending on the cyclic shear strain amplitude there is a stable, metastable and unstable region, which can be explained with the shear strain threshold concept (Vucetic 1994). The regions could also be differentiated by their failure mode such as stabilization, shakedown and progressive failure, respectively.

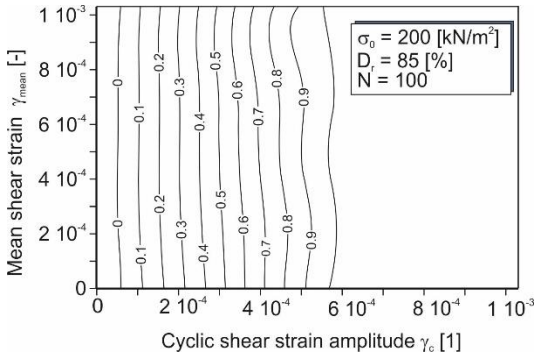

Figure 5. Excess pore pressure ratio isolines for mean and amplitude shear strain after 100 cycles for S30T.

The normalized excess pore pressure for different shear strain amplitudes is plotted against the number of cycles in log-scale in Figure 6. Curve 5 only accumulates small amounts of excess pore pressure. Curve 1 fails after a few cycles as it is accumulating and progressing to failure; whereas curves 3 - 4 are accumulating excess pore pressure steadily for a large number of cycles in log-scale. Curve 4 seems to be metastable and accumulate some excess pore pressure without a progressing failure trend. The incremental change for curve 5 between 100 and 1000 cycles is recognizable in log-scale but comparatively small. For these amplitudes the excess pore pressure has build-up and the shear modulus is degraded for only a limited number of cycles. Similar behaviour was reported for instance by Lefebvre et al. (1989) and Drnevich et al. (1967).

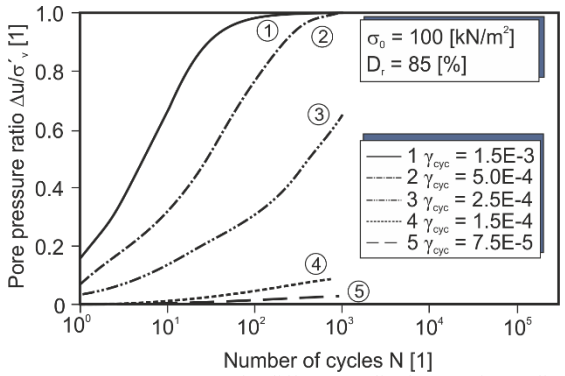

Figure 6. Excess pore pressure for different cyclic shear strain amplitudes against number of cycles for S30T.

The shear strain amplitude of curve 5 in Figure 6 is the smallest shear strain of all curves. The soil response for small shear strain amplitudes can be found in Figure 7, as well. Figure 7 shows the excess pore pressure build-up after different number of cycles for a vertical stress of 100 kPa. It can be seen that all curves start of a specific value and then steadily start to deviate. Liquefaction is reached for different number of cycles at different shear strain amplitudes. For an increasing number of cycles this value decreases, because more excess pore pressure accumulates over time.

High excess pore pressures are generated after only several cycles for high cyclic shear strain amplitudes and low vertical stresses (Figures 7 and 8). Thus, for a higher vertical effective stress and the same number of cycles the liquefaction shear strain

value increases (Figure 8). For higher shear strains larger degradation of the soil and a softer soil response arises. The contractive soil behaviour is more pronounced for this softer behaviour and larger plastic strains.

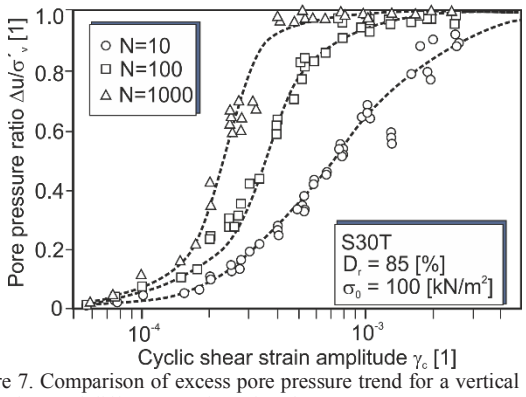

Figure 7. Comparison of excess pore pressure trend for a vertical stress of 100 kPa and different number of cycles (D_r = 0.85).

The influence of the vertical stress for the same number of cycles can be seen when comparing different vertical stresses in Figure 8. Two different vertical stresses are compared for the normalized excess pore pressure over the shear strain amplitude. The state of total liquefaction is reached at two different shear strains after the same number of cycles. The starting value of accumulation (volumetric threshold) increases for higher stresses. The calculated volumetric thresholds are also depicted in Figure 8. The calculative criterion is explained later. The stress dependency of the volumetric threshold can clearly be seen. The soil response and generation of excess pore pressure is directly correlatable with the softening of the sample and hence the degradation of shear modulus. This on the other hand is correlated to the shear strain (and also the increase in damping). The stiffer soil behaviour can also be recognized by the stress-dependent shear modulus. Due to higher stresses larger shear strains are necessary to induce a similar damage as for the case of lower stresses. To reach a similar "damage" for the same shear strain, larger number of cycles are needed.

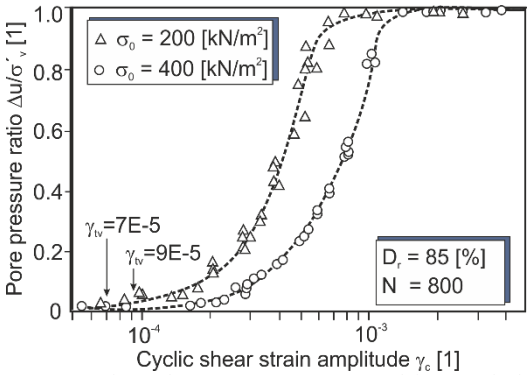

Figure 8. Comparison of excess pore pressure trend for a vertical stress of 200 kPa and 400 kPa for 800 cycles (D_r = 0.85).

Figure 9 shows the influence of different relative densities for two different stress levels for S30T after 100 cycles. The influence of the relative density is not very pronounced, but seems to be larger for 100 kPa than for 400 kPa vertical effective stress. This agrees well with the findings of the literature (e.g. Dobry et al. (1985)).

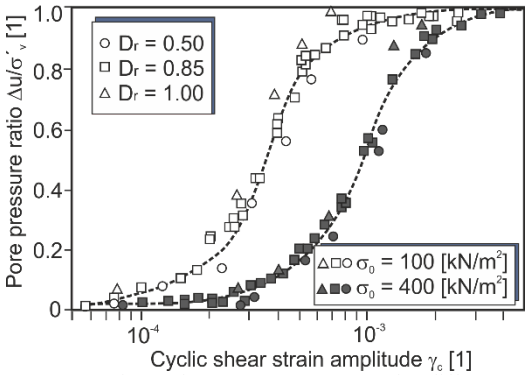

Figure 9. Comparison of excess pore pressure for different relative densities after 100 cycles for S30T sand and two vertical stresses.

The number of cycles to liquefaction N_{liq} is especially important when dealing with liquefaction problems (Seed 1976). Figure 10 shows this value dependent on the shear strain amplitude for different vertical stresses. For a high number of cycles a stable stress-dependent shear strain value (volumetric threshold) can be seen. The shear strains for a small number of cycles to liquefaction have been extrapolated based on a power function regression. A stress dependency of the general soil response is evident.

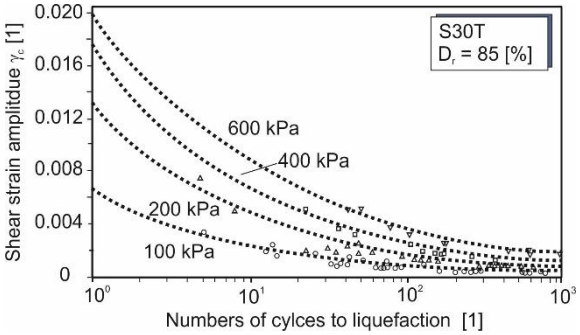

Figure 10. Shear strain amplitude over number of cycles to liquefaction for S30T for different vertical stresses (D_r = 0.85).

4 CONCEPT

The data were plotted in a three-dimensional representation for a vertical stress of 200 kPa. Figure 11 shows the general soil response for different shear strain amplitudes and for different number of cycles. The black lines represent results from cyclic direct simple shear tests and the coloured plane bases on a performed regression analysis. Herein, it was important to fit small and large values as well as the metastable region well. The shape depends on the vertical stress and the specific soil. The relative density only partially influences the given shape. However, for a new material the shape shall be easily derivable from only a limited number of laboratory tests.

The empirical regression plotted in Figure 11 bases on an exponential approach up to the degradation threshold and a subsequent hyperbolic tangent function. Hence, there is a change in inclination at $\tilde{\gamma}_{td}$. No accumulation of excess pore pressure is expected below the volumetric threshold (Figure 12). The degradation threshold was fitted over the vertical stresses. The hyperbolic tangent function was fitted over the number of cycles and the vertical stresses. The latter was also fitted over the shear strain amplitudes.

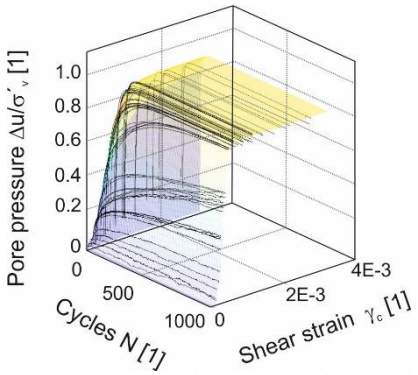

Figure 11. Overview of test results for S30T with a vertical stress of 200 kPa for excess pore pressure over number of cycles and shear strain amplitude (log-scale) (D_r = 0.85).

The degradation threshold describes the shear strain from which a shakedown failure is initiated. Figure 12 shows a slice of the three-dimensional plot for a number of cycles of 50. The volumetric and degradation threshold are also depicted.

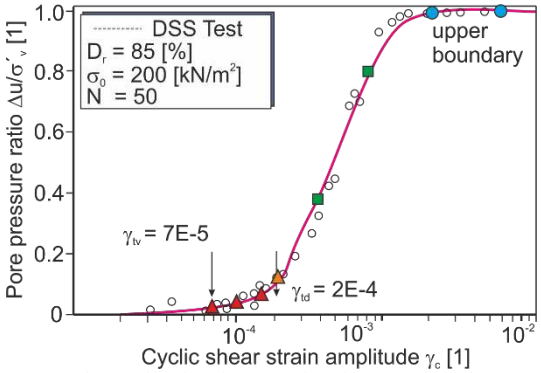

Figure 12. Advanced estimation equation for N = 50, D_r = 0.85 and vertical stress of 200 kPa.

Based on all results, the volumetric thresholds were extracted from the direct simple shear tests and correlated to the location within the shear modulus degradation curve. This was also done for the degradation threshold. The volumetric threshold was taken at 2% excess pore water pressure after 1000 cycles.

The results of the cyclic direct simple shear test have been processed with an approach similar to the approach from to Hsu et Vucetic (2004) to derive $\tilde{\gamma}_{td}$. The degradation threshold was taken, where the average secant shear modulus decreases by 0.5%. Therefore, the secant shear modulus for different number of cycles is normalized with the shear modulus in the first cycle. Subsequently, the inclination is estimated by using a logarithmic regression applied to the normalized secant shear modulus plotted against the number of cycles (Figure 13 left). The parameter t is an indicator for the average variance of the shear modulus over the number of cycles. This procedure was applied to all individual test phases. A curve with t = 0 (δ = 1) represents no degradation of the number of cycles (Figure 13 left) and implies that the test has been performed for a value smaller than the volumetric threshold. After the volumetric threshold a gradual decrease in the shear modulus occurs as the microstructure is irreversibly altered and permanent deformations occur. The degradation threshold $\tilde{\gamma}_{td}$ was defined herein as a slope of 0.5% (Figure 13 right). This value was analysed in a sensitivity study and led to the best results.

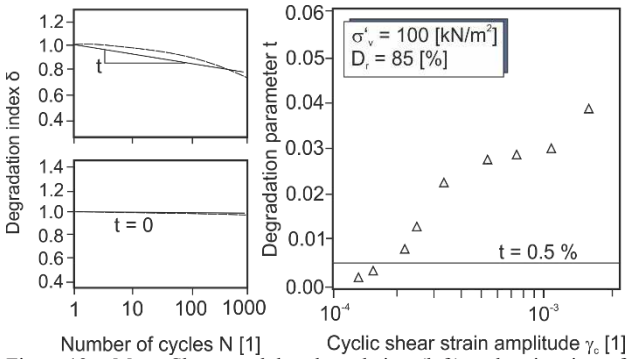

Figure 13. Mean Shear modulus degradation (left) and estimation of degradation threshold based on Hsu et Vucetic (2004) (right).

The derived thresholds were then compared to results from Resonant Column tests. The volumetric shear strain could be located at 0.95 G/G_0 and the degradation threshold at 0.85 G/G_0. Figure 14 shows the test data and also the location of the different thresholds. All findings have been verified by using three additional sandy soils. The shear strain amplitude for 0.95 and 0.85 G/G_0 could be read from a shear modulus degradation curve based on a regression analysis from Resonant Column results (for instance with the equation according to Santos et Correia 2001). An additional direct simple shear test at the degradation threshold derived from RC results is necessary due to plastic deformation and a dependency over the number of cycles (cf. Figure 7 at γ = 0.016%). The octahedral stress state from the Resonant Column test can be transferred to a theoretical vertical effective stress with the coefficient of earth pressure at rest. However, a more convenient way is to use multistage direct simple shear tests (MCDSS) for different shear strain values and evaluate γ_{tv} and γ_{td} afterwards. By using MCDSS tests the needed test results are directly present.

For very small shear strain amplitudes, no plastic deformation is expected. The first elastoplastic response is predicted at γ_{tv}. Hence, multistage tests can be used up to at least $\gamma_{tv,}$ because up to this value only marginal plastic deformations occur. In order to reduce the laboratory effort further, the results up to $\tilde{\gamma}_{td}$ can be accepted including an error between γ_{tv} and $\tilde{\gamma}_{td}$ due to the known plastic soil response. The error depends on the amount of tests between these two values. This procedure is shown in Figure 12 with triangles up to γ_{tv} and the last triangle representing $\tilde{\gamma}_{td}$; all obtained in a MCDSS. This procedure is an estimation approach in order to optimize the laboratory effort and derive the soil response with the least effort.

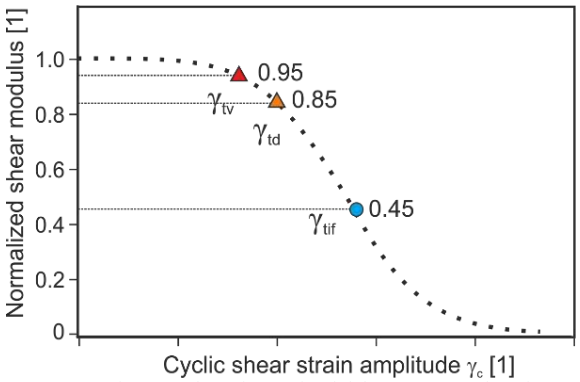

Figure 14. Basic procedure for optimal laboratory test location with rough location of shear strain thresholds within the normalized shear modulus reduction curve.

The upper shear strain value $\tilde{\gamma}_{tif}$, indicated with a filled circle, can be estimated from Resonant Column tests at 0.45 G/G_0. The value of 0.45 G/G_0 was derived based on the laboratory results and was chosen in a way that a progressive liquefaction failure occurs in the sample. Between the upper value and the degradation threshold additional tests can optionally be placed in equidistance in log-scale (squares in Figure 12). The locations of the thresholds are schematically presented in Figure 14.

Figure 15 shows the results of the presented procedure. The excess pore pressure build-up from a cyclic constant-volume direct simple shear test under displacement-controlled conditions is depicted. Five tests are used to define the characteristic shape. The results of the multistage tests cover the shear strain amplitudes up to the degradation threshold (red curves). The small deviation due to plastic deformations within a multistage test can be neglected due to the economic reduction of time and costs for additional single-stage tests. The initial failure line for a shear strain $\tilde{\gamma}_{tif}$ is plotted in blue and was derived from fitted RC results. These curves are performed with larger shear strains and show a progressive failure and hence an upper boundary. The green curves have been derived with direct simple shear tests with strain amplitudes between the red and blue curves with an equivalent logarithmic distance. The results can be compared with the same colour pattern with Figures 12 and 14.

Instead of fitting the curves with an empirical equation, the test results can linearly be interpolated, because the positions of the single tests lay on all characteristic points within the S-shape of the soil response (Figure 12).

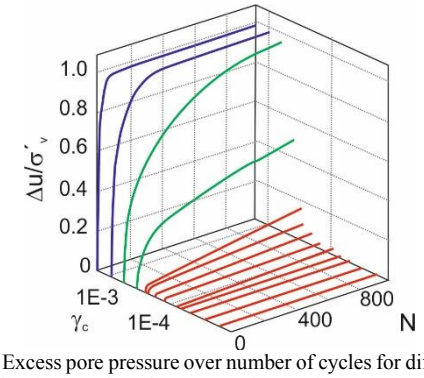

Figure 15. Excess pore pressure over number of cycles for different shear strain amplitudes based on the presented procedure.

5 CONCLUSION

The general soil response under cyclic displacements was presented for a reference soil. The presented investigation shows high potential to help understanding the soil response under cyclic loading in greater detail and can be used as a basis to estimate the influence of excess pore pressure build-up of various offshore foundations.

The derived concept can be used for an optimal distribution of laboratory tests and for different approaches in order to calculate the excess pore pressure due to cyclic loading with displacement-controlled characteristics. It should be mentioned that for offshore conditions soil responses for more than a few dozen cycles are necessary and need to be determined as accurately as possible. However, on the other hand the accumulation for smaller shear strains, which do not lead to full liquefaction, can influence the integrity of the structure. The presented procedure is capable of predicting both boundary conditions.

The gained knowledge will be used and adapted for tests with stress-based approaches to be developed. Furthermore, it can serve as a database for the calibration of higher-quality constitutive laws or as a first reference point for poorly-grained sands with round particles.

6 ACKNOWLEDGEMENTS

The investigations reported were partially funded by the Deutsche Forschungsgemeinschaft (DFG, German Research Foundation) - SFB1463 – 434502799. The support is gratefully acknowledged.

7 REFERENCES

Achmus, M., Saathoff, J.-E., Thieken, K. (2018). Numerical method for evaluation of excess pore pressure build-up at cyclically loaded offshore foundations, Proceedings of the 24th NumGe, Vol. 2.

Díaz-Rodríguez, J.A. and López-Molina, J.A (2008). Strain thresholds in soil dynamics. The 14th World Conference on Earthquake Engineering. October 12-17, 2008, Beijing, China.

Dobry, R. (1985). Liquefaction of soils during earthquakes. Rep. No. CETS-EE-001, National Research Council (NRC), Committee on Earthquake Engineering, Washington, DC.

Dobry, R., Ladd, R. S., Yokel, F. Y., Chung, R. M., and Powell, D. (1982). Prediction of pore-water pressure buildup and liquefaction of sands during earthquakes by the cyclic strain method." National Bureau of Standards Building Science Series 138, National Bureau of Standards, U.S. Dept. of Commerce, Washington, D.C.

Drnevich, V.P. (1967). Effects of strain history on the dynamic properties of sand. Thesis. University of Michigan.

Dyvik, R., Berre, T., Lacasse, S. and Raadim, B. (1987). Comparison of truly undrained and constant volume direct simple shear tests. Géotechnique 37:1, 3-10.

Feda, J (1971). Constant volume shear tests of saturated sand. Archiv. Hydrot. 18, No. 3, 349-367.

Finn W.D.L. and Y.P. Vaid. (1977). Liquefaction Potential from Drained Constant Volume Cyclic Simple Shear Tests, In Proceedings of the Sixth World Conference on Earthquake Engineering, Indian Society of Earthquake Technology, Neu Delhi, 2157-2162.

Hsu. C.C. and Vucetic M. Volumetric (2004). Threshold Shear Strain for Cyclic Settlement. Journal of Geotechnical and Geoenvironmental Engineering, Vol. 130, No. 1, January 1.

Lefebvre, G.S., Leboeuf, D., and Demers, B. (1989). Stability threshold for cyclic loading of saturated clay. Canadian Geotechnical Journal 26 (1): 122-131.

Okur, D.V. and Ansal, A. (2007). Stiffness degradation of natural fine-grained soils during cyclic loading. Soil Dynamics and Earthquake Engineering 27: 843-854.

Saathoff, J.-E. and Achmus, M. (2020). Practical approach for the evaluation of cyclically induced excess pore pressure around offshore foundations in sand. 4th International Symposium on Frontiers in Offshore Geotechnics, Texas.

Santos, J.A., and Correia, A.G. (2001). Reference threshold shear strain of soil and its application to obtain a unique strain-dependent shear modulus curve for soil. Proceedings of the 15th International Conference on Soil Mechanics and Geotechnical Engineering, 267-270.

Seed, H. B. (1976). Evaluation of Soil Liquefaction Effects of Level Ground During Earth-quakes, Presented at the ASCE Annual Convention and Exposition, Philadelphia, Pa., Sept. 27-0ct. l.

Silver, M. L., and Seed, H. B. (1971). Volume changes in sands during cyclic loading. J. Soil Mech. Found. Div., 97(9), 1171–1182.

Vucetic M and Mortezaie, A.M. (2015). A Cyclic secant shear modulus versus pore water pressure in sands at small cyclic strains, Soil Dynamics and Earthquake Engineering, 70.

Vucetic, M. (1994). Cyclic threshold shear strains in soils, J. Geotech. Engrg., ASCE,120 (12), 2208-2228 156.

Wichtmann T. and Triantafyllidis, T. (2010). On the influence of the grain size distribution curve on P-wave velocity, constrained elastic modulus Mmax and Poisson's ratio of quartz sands. Soil Dynamics and Earthquake Engineering, 30(8):757-766.

Wichtmann, T. and Triantafyllidis, T. (2013). Effect of uniformity coefficient on G=Gmax and damping ratio of uniform to well-graded quartz sands. Journal of Geotechnical and Geoenvironmental Engineering Vol. 139(1), 59-72.